GEOPHYSICAL RESEARCH LETTERS, VOL. 22, NO. 3, PAGES 283-286, FEBRUARY 1, 1995

Regional estimation of electric fields and currents in the polar ionosphere

Mariko Sato,[1] Y. Kamide,[1] A.D. Richmond,[2] A. Brekke,[3] and S. Nozawa[1]

Abstract. A new technique is presented to estimate electric fields and currents in a localized region of the high-latitude ionosphere by combining two magnetogram-inversion algorithms. This paper describes the concept and practical procedures of the method as well as the first results of our efforts in which this new scheme is applied to northern Scandinavia, computing the ionospheric parameters on a small scale. Examining latitudinal profiles of these parameters and precipitating particles, it is found that the region of the most intense precipitation in the morning sector is located equatorward of the region of the strongest electric field. To evaluate the relative importance of ionospheric and magnetospheric effects, the field-aligned current is divided into two components: $(\nabla\Sigma)\cdot\mathbf{E}$ and $\Sigma\nabla\cdot\mathbf{E}$. These two components give often the opposite directions in the resultant field-aligned currents. The relative strength of the two components appears to vary considerably with latitude.

Introduction

The global convection and current patterns have extensively been discussed with advanced magnetogram-inversion schemes: see review by *Kamide and Baumjohann* [1993]. KRM (Kamide, Richmond and Matsushita; *Kamide et al.*, 1981) and AMIE (Assimilative Mapping of Ionospheric Electrodynamics; *Richmond and Kamide*, 1988) techniques have been used in estimating ionospheric electric fields, currents and field-aligned currents over the entire polar region. However, since the "action" region during individual substorms is restricted to a rather limited area, detailed studies of electrodynamic parameters on a smaller scale are necessary to better understand substorm dynamics. In spite of such acute necessity, only the global patterns of ionospheric properties have so far been addressed in most of the earlier studies based on the magnetogram-inversion method.

As one of the few exceptions, *Murison et al.* [1985] applied a magnetogram-inversion scheme to data from the Scandinavian Magnetometer Array (SMA). Since relatively simple conductance models and boundary conditions were employed, however, their results included some unrealistic distribution of the electric potential. *Inhester et al.* [1992] used SMA magnetic data and electric field information from the STARE radar as input to attempt to solve a first-order differential equation for the Hall conductance. Although the STARE observations played a major role in their attempt, the coverage in the ionosphere by the radar was limited, so that the electric field had to be extrapolated in some regions. See *Untiedt and Baumjohann* [1993] for important issues concerning this point.

This paper presents the first result of estimating ionospheric quantities by combining the AMIE and KRM algorithms for (1) realistic boundary conditions for the current function and the electric potential and for (2) realistic conductance distributions. In this way, it is hoped that it becomes possible to estimate the ionospheric parameters on a small scale and to examine their mutual spatial relationship.

Data and Procedure

The first step of the practical calculation is to estimate the ionospheric current function from magnetometer data. Magnetometer data for the regional estimation come from 17 stations in northern Scandinavia, whose locations are shown in Fig. 1. To specify the boundary condition for solving an equation in terms of the current function, the global distribution of the current function is obtained from the AMIE technique. The grid size for global AMIE runs is 1.7° and 10° in latitude and longitude, respectively. Magnetometer data from 81 stations in the northern hemisphere are used for this AMIE calculation.

The distribution of the Hall and Pedersen conductances is required as input for the KRM algorithm. By using the approximate formula of *Robinson et al.* [1987], the conductances resulting from auroral particle precipitation can be estimated from the energy flux and average energy of precipitating electrons measured by the DMSP (Defence Meteorological Satellite Program) satellite. It takes about 4 minutes for DMSP-F8 to pass over the region. We also use electron densities obtained by EISCAT (European Incoherent Scatter) CP-1 measurements to deduce the conductances (*Brekke and Hall*, 1988). In the present study, we assume for simplicity that the conductances are longitudinally homogeneous outside the region which satellite and radar measurements cover.

Once the current function is calculated in the localized area, the electric potential distribution can be obtained by solving a second-order differential equation with the specified Hall and Pedersen conductances. The boundary condition for this differential equation is also given by the global AMIE calculation for the electric potential. We then solve the equation over a grid with 1° and 2° spacing in the magnetic latitude and longitude, respectively. Vectors of the electric field and of the horizontal current are calculated from the electric potential. Field-aligned currents are derived by taking the divergence of the ionospheric current.

Examples of the regional estimation in the morning sector

We have applied the new scheme to several substorms. We present in this paper a case for 0320 UT on April 10, 1990, where the DMSP satellite passed

[1] Solar-Terrestrial Environment Laboratory, Japan

[2] High Altitude Observatory, NCAR, Boulder, CO

[3] Auroral Observatory, Norway

Paper number 94GL03076
0094-8534/95/94GL-03076$03.00

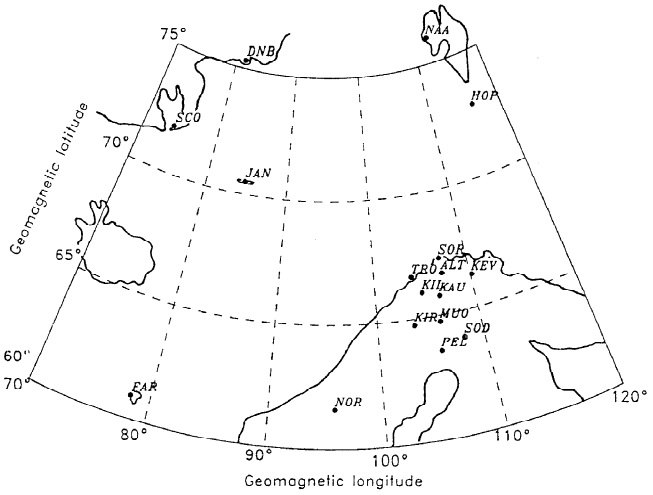

Figure 1. Map showing the magnetometer stations whose data are used for the regional estimation in the present study. The EISCAT radar, of which data are used to deduce the electric field and the conductances, is located near Tromsø (TRO).

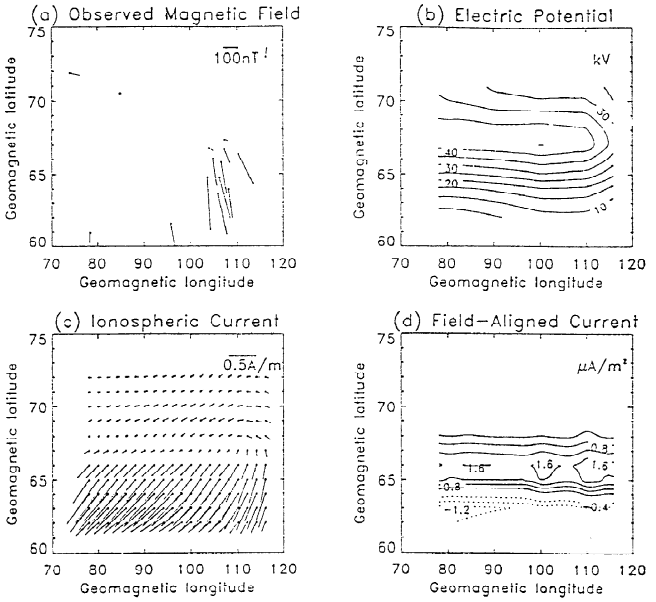

Figure 2. (a) Observed magnetic perturbation vectors at 0320 UT. (b) Estimated electric potential. (c) Horizontal current vectors calculated from the electric fields and the Hall and Pedersen conductances. (d) Isointensity contours of the calculated field-aligned current. Solid lines represent downward currents and dotted lines are for upward currents.

over the EISCAT radar near the 106° magnetic meridian. Two substorms of nearly the same intensity in AL ($= -500$ nT) before (around 0100 UT) and after (0430 UT) this pass time. Fig. 2 (a) shows magnetic perturbation vectors observed at the stations shown in Fig. 1. Magnetic disturbances as large as -400 nT can be seen between 63° and 66°.

In order to compare a electric potential pattern derived from the regional estimation, shown in Fig. 2(b), with a global pattern, we show in Fig. 3 the electric potential over the entire polar region. The distribution of the conductances for this global calculation is determined by a model of *Ahn et al.* [1983], which uses the empirical relationship between the conductances and ground magnetic perturbations. A thick line in Fig. 3 represents the boundary of the region in which electrodynamic parameters are to be estimated for northern Scandinavia.

In Fig. 2 (b), the boundary which separates the northward and southward electric fields is clearly seen at 68° magnetic latitude, while that boundary is less clear in Fig. 3. It is probable that this boundary indicates the poleward boundary of the westward electrojet. Southward electric fields peak at about 65°, which becomes one of the important loci when we discuss spatial relationships between the electric field and the conductances later in this paper.

Figs. 2 (c) and (d) present ionospheric current vectors and isointensity contours of field-aligned currents, respectively. The auroral electrojet flows southwestward and the peak current density is ~ 0.4 A/m. Between 64° and 69° the field-aligned current flows downward, and an upward current is located equatorward of the downward current. It may well be that this represents the well-known field-aligned current configuration in this local time section, i.e., region 1 and region 2. The maximum intensity of the downward current is 1.8 μA/m^2 (integrated value along the meridian being 0.5 A/m) and that of the upward current is 1.2 μA/m^2 (0.3 A/m).

Latitudinal profile of the ionospheric parameters

The relative distribution of the ionospheric currents, the Hall conductance and the electric field is shown in Fig. 4(a). Electric fields observed by DMSP and EISCAT and currents deduced from the EISCAT measurements are also shown to verify the validity of our calculation. It is seen that the calculated electric fields and the height-integrated currents are in reasonable agreement with the values obtained by DMSP and by EISCAT.

It is evident that the region of the highest conductance is located equatorward of that of the strongest

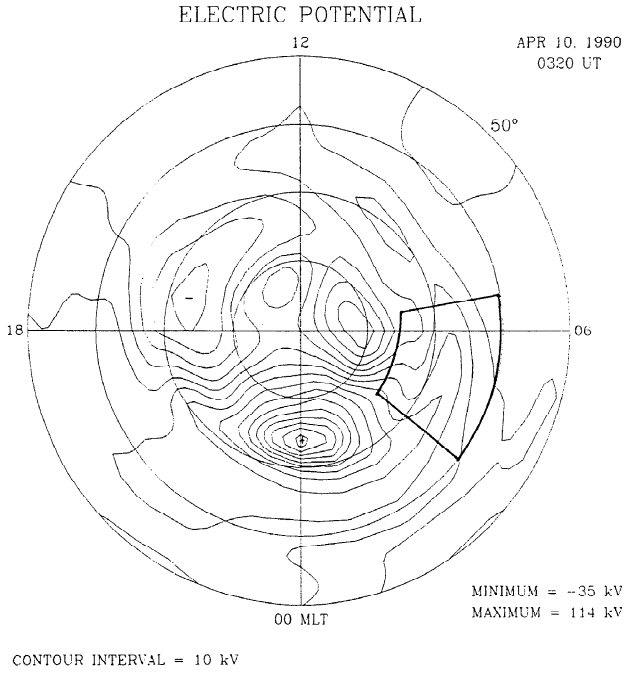

Figure 3. Electric potential patterns over the entire polar region at 0320 UT obtained by the KRM algorithm.

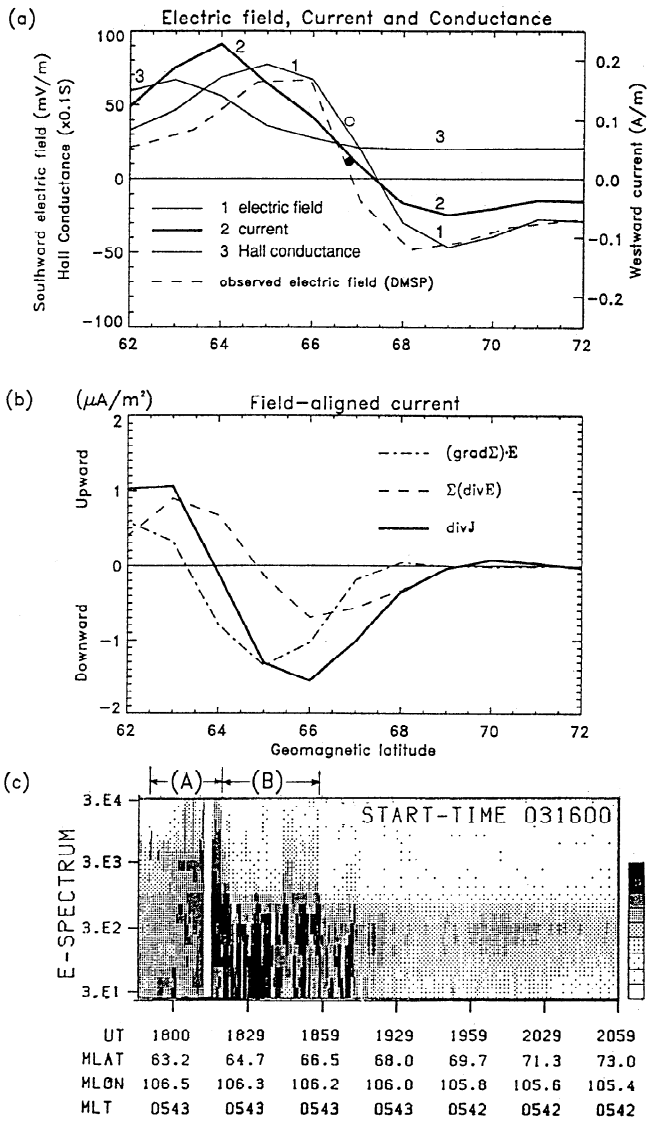

Figure 4. (a) Comparison between the calculations and measurements for the southward electric field and the westward current. The observed electric field along a DMSP orbit is also shown. The open and solid circles indicate the southward electric field and the westward current respectively observed by EISCAT. (b) Latitudinal profiles of the estimated field-aligned currents (solid line). The contribution of nonuniformities of the conductance ($(\nabla\Sigma)\cdot\mathbf{E}$) and that of the divergence of electric fields ($\Sigma\nabla\cdot\mathbf{E}$) to the net field-aligned current are shown separately. (c) Energy-time spectra of precipitating electrons observed by DMSP-F8.

electric field. This implies that roles of the conductance and the electric field vary with latitude, and that the conductances are dominant in generating the electrojet in the equatorward half of the electrojet, and vice versa. These characteristics are consistent with earlier observations of electric fields, currents and conductances by radars [e.g., *Kamide and Vickrey*, 1983].

It is worth noting that the lack of correspondence between the peak of the ionospheric conductance and that of the electric field can also be seen in another example under more disturbed conditions at 0500 UT on the same day (not shown in this paper), where an intense westward electrojet (1.4 A/m at the center of the electrojet) was observed. In that region, where the Hall conductance (~ 25 S) was very high, the electric field (~ 50 mV/m) was smaller than that of 0320 UT(~ 70 mV/m). This indicates that the electric field may become small where the conductances are relatively high. One of the implications of this feature is that the meridional electric fields in the morning sector may be decomposed into an "ambient" convection electric field and an "aurora-associated" field, whose directions are opposite to each other (see *Baumjohann*, 1983).

The relationship between field-aligned currents and particle precipitation

Figs. 4 (b) and (c) show, respectively, the latitudinal extent of the field-aligned current and energy-time spectra of precipitating electrons observed by DMSP. Electrons with relatively high energies (5–10 keV), which are often seen in the morning sector [e.g., *Lyons and Fennell*, 1986], are observed equatorward of 64.2° (labeled as A), enhancing the Hall conductance more effectively than the Pedersen conductance. This electron region coincides with the upward-current region. Note that electrons with low energies and large fluxes (0.1 erg/cm^2/sr/sec) precipitate in the downward current region (labeled as B).

It is also noticeable from Figs. 4 (a) and (b) that the boundary between the upward and downward currents is not located at the point where the electric field is maximum but is shifted equatorward.

In order to understand the relationship between the field-aligned current and precipitating particles, it is of interest to examine relative roles of the conductance gradient and the divergence of electric fields in generating the field-aligned currents. Their contributions to the net field-aligned current ($=\nabla\cdot\mathbf{J}$) are shown in Fig. 4(b). $(\nabla\Sigma)\cdot\mathbf{E}$ is the ionospheric origin field-aligned current [Boström, 1974] due to nonuniformities of ionospheric conductances, while $\Sigma\nabla\cdot\mathbf{E}$ represents the magnetospheric origin currents. It is clear that the relative contribution of $(\nabla\Sigma)\cdot\mathbf{E}$ and $\Sigma\nabla\cdot\mathbf{E}$ to the net current changes significantly, depending on the latitude, and that there is a region where $(\nabla\Sigma)\cdot\mathbf{E}$ and $\Sigma\nabla\cdot\mathbf{E}$ currents flow in the opposite directions. At the equatorward portion of the downward current (64°–65°), the downward current due to ionospheric conductance nonuniformities exceeds in intensities the upward current generated by $\Sigma\nabla\cdot\mathbf{E}$. That is, the downward current can flow even in the region where div **E** is negative.

Sugiura [1984] pointed out that the sign of div **E** and the flow direction of the field-aligned current (downward is positive) coincide well in the dayside where the spatial distribution of the ionospheric conductances are fairly uniform. Our result shows that conductance nonuniformities can play an important role in generating the field-aligned current, especially at the equatorward part of the downward current. This is why the upward/downward currents boundary is not located at the peak of the electric field. As described above, auroral particles with enhanced energy fluxes precipitate in the region, where div **E** is negative but the net current is downward. It appears that the upward flow of electrons are carrying the downward current in this complicated region.

Conclusion

On the basis of a new scheme outlined in this paper, we have been able to estimate ionospheric parameters on a small scale. It is found that the region of

the most intense precipitation is located equatorward of the region of the strongest electric field. By considering two components of the field-aligned current, this feature is interpreted in the following way: The region of the upward field-aligned current which relates to the divergence of the electric field is located equatorward of the peak of the southward electric field. This upward current region is embedded in electrons with intense energy fluxes. In particular, an average energy is relatively high (several keV) in this equatorward portion. The resultant nonuniformities of the ionospheric conductances are in charge of the ionospheric origin downward current and this can exceed the upward current derived by $\Sigma\nabla \cdot \mathbf{E}$ near the boundary separating high- and low-average energies of precipitating particles. In other words, the field-aligned current can flow downward in the region where the divergence of the electric field is negative.

The characteristics of the relative function of the electric field and the conductance are extremely important in unveiling substorm mechanisms. One of the outstanding problems for substorms is to clarify temporal changes of the current systems throughout the growth and decay of substorms. It will be possible, by using our new scheme presented in this paper, to examine quantitatively the relative importance of the ionospheric conductance and the electric field in generating the horizontal currents as well as the field-aligned currents for the different substorm phases. Although in the present study, we have shown the results of our application to data only in the morning sector, a study is underway in which this new scheme is being applied to the midnight sector, where more localized structures are present.

Acknowledgments. One of the authors (M.S.) would like to thank the High Altitude Observatory for its financial support and hospitality during her stay in the summer of 1993. EISCAT is a scientific association supported by the research councils of Finland, France, Germany, Norway, Sweden, and the United Kingdom. The work at STEL was supported in part by The Scandinavia-Japan Sasakawa Foundation. The work of M.S. was supported by the Research Fellowships program of the Japan Society for the Promotion of Science for Young Scientists.

References

Ahn, B.-H., R.M. Robinson, Y. Kamide, and S.-I. Akasofu, Electric conductivities, electric fields and auroral particle energy injection rate in the auroral ionosphere and their empirical relations to the horizontal magnetic disturbances, *Planet. Space Sci., 31*, 641–653, 1983.

Baumjohann, W., Ionospheric and field-aligned current systems in the auroral zone: A concise review, *Adv. Space Res., 2*, 55–62, 1983.

Boström, R., Ionosphere-magnetosphere coupling, in *Magnetospheric Physics*, edited by B.M. McCormac, pp. 45–59, D. Reidel, Hingham, Mass., 1974.

Brekke, A. and C. Hall, Auroral ionospheric quiet summer time conductances, *Ann. Geophysicae, 6*, 361–376, 1988.

Inhester, B., J. Untiedt, M. Segatz, and M. Kürschner, Direct determination of the local ionospheric Hall conductance distribution from two-dimensional electric and magnetic field data, *J. Geophys. Res., 97*, 4073–4083, 1992.

Kamide, Y., and W. Baumjohann, *Magnetosphere-Ionosphere Coupling*, Springer-Verlag, Heidelberg, 1993.

Kamide, Y., and J.F. Vickrey, Relative contribution of ionospheric conductivity and electric field to the auroral electrojets, *J. Geophys. Res., 88*, 7989–7996, 1983.

Kamide, Y., A.D. Richmond and S. Matsushita, Estimation of ionospheric electric fields, ionospheric currents and field-aligned currents from ground magnetic records, *J. Geophys. Res., 86*, 801–813, 1981.

Lyons, L.R. and J.F. Fennell, Characteristics of auroral electron precipitation on the morningside, *J. Geophys. Res., 91*, 11225–11234, 1986.

Murison, M., A.D. Richmond, S. Matsushita, and W. Baumjohann, Estimation of ionospheric electric fields and currents from a regional magnetometer array, *J. Geophys. Res., 90*, 3525–3530, 1985.

Richmond, A.D., and Y. Kamide, Mapping electrodynamic features of the high-latitude ionosphere from localized observations: Technique, *J. Geophys. Res., 93*, 5741–5759, 1988.

Robinson, R.M., R.R. Vondrak, K. Miller, T. Dabbs, and D. Hardy, On calculating ionospheric conductances from the flux and energy of precipitating electrons, *J. Geophys. Res., 92*, 2565–2569, 1987.

Sugiura, M., A fundamental magnetosphere-ionosphere coupling mode involving field-aligned currents as deduced from DE-2 observations, *Geophys. Res. Lett., 9*, 877–880, 1984.

Untiedt, J. and W. Baumjohann, Studies of polar current systems using the IMS Scandinavian magnetometer array, *Space Sci. Rev., 63*, 245–390, 1993.

Mariko Sato, Y. Kamide and S. Nozawa,
Solar-Terrestrial Environment Laboratory, Nagoya University, 3–13 Honohara, Toyokawa, Aichi, Japan

A.D. Richmond, High Altitude Observatory, National Center for Atmospheric Research, P. O. Box 3000, Boulder, CO 80307

A. Brekke, Auroral Observatory, University of Tromsø, N–9037 Tromsø, Norway

(received August 23, 1994; accepted November 04, 1994.)